Title

Peroxisome proliferator-activated receptor delta limits the expansion of pathogenic Th cells during central nervous system autoimmunity.

Journal

The Journal of experimental medicine, 207(8)

ISSN

0022-1007

Authors

Dunn, Shannon E
Bhat, Roopa
Straus, Daniel S
et al.

Publication Date

2010-08-01

DOI

10.1084/jem.20091663

Peer reviewed

Peroxisome proliferator–activated receptor δ limits the expansion of pathogenic Th cells during central nervous system autoimmunity

Shannon E. Dunn,[1,6] Roopa Bhat,[1] Daniel S. Straus,[5] Raymond A. Sobel,[2] Robert Axtell,[1] Amanda Johnson,[1] Kim Nguyen,[1] Lata Mukundan,[3] Marina Moshkova,[6] Jason C. Dugas,[4] Ajay Chawla,[3] and Lawrence Steinman[1]

[1]Department of Neurology and Neurological Sciences, [2]Department of Pathology, [3]Department of Medicine, Division of Endocrinology, and [4]Department of Neurobiology and Developmental Biology, Stanford University, Stanford, CA 94305
[5]Division of Biomedical Sciences, University of California, Riverside, Riverside, CA 92501
[6]University Health Network, Toronto, ON M5G 2C4, Canada

Peroxisome proliferator–activated receptors (PPARs; PPAR-α, PPAR-δ, and PPAR-γ) comprise a family of nuclear receptors that sense fatty acid levels and translate this information into altered gene transcription. Previously, it was reported that treatment of mice with a synthetic ligand activator of PPAR-δ, GW0742, ameliorates experimental autoimmune encephalomyelitis (EAE), indicating a possible role for this nuclear receptor in the control of central nervous system (CNS) autoimmune inflammation. We show that mice deficient in PPAR-δ (PPAR-$\delta^{-/-}$) develop a severe inflammatory response during EAE characterized by a striking accumulation of IFN-γ^{+}IL-17A^{-} and IFN-γ^{+}IL-17A^{+} CD4^{+} cells in the spinal cord. The preferential expansion of these T helper subsets in the CNS of PPAR-$\delta^{-/-}$ mice occurred as a result of a constellation of immune system aberrations that included higher CD4^{+} cell proliferation, cytokine production, and T-bet expression and enhanced expression of IL-12 family cytokines by myeloid cells. We also show that the effect of PPAR-δ in inhibiting the production of IFN-γ and IL-12 family cytokines is ligand dependent and is observed in both mouse and human immune cells. Collectively, these findings suggest that PPAR-δ serves as an important molecular brake for the control of autoimmune inflammation.

CORRESPONDENCE
Shannon Dunn:
sdunn@uhnresearch.ca
OR
Lawrence Steinman:
steinman@stanford.edu

Abbreviations used: CNS, central nervous system; EAE, experimental autoimmune encephalomyelitis; MOG, myelin oligodendrocyte glycoprotein; PPAR, peroxisome proliferator–activated receptor; RXR, 9-cis retinoic acid receptor.

Pathogenic Th1 and Th17 cells specific for myelin autoantigens are regarded as critical for both initiation and perpetuation of inflammation in multiple sclerosis and its animal model, experimental autoimmune encephalomyelitis (EAE; Diveu et al., 2008). Cytokines involved in the Th1 and Th17 axes of inflammation are detected in active lesions of multiple sclerosis patients (Windhagen et al., 1995; Lock et al., 2002; Kebir et al., 2009) and in the central nervous system (CNS) of mice with EAE (Langrish et al., 2005). Adoptive transfer studies indicate that both Th1 and Th17 cells can initiate the autoimmune cascade in this disease (Stromnes et al., 2008; Kroenke et al., 2008).

Peroxisome proliferator–activated receptors (PPARs) are members of the nuclear hormone receptor superfamily. This group of ligand-activated transcription factors regulates diverse processes including lipid and glucose homeostasis, cell proliferation and differentiation, and inflammation (Straus and Glass, 2007). PPARs are considered to be nutritional sensors, as they are bound and activated by fatty acid intermediates and can thus translate lipid levels into altered gene transcription. PPAR-γ binds oxidized and nitrosylated fatty acids as well as certain eicosanoids and prostaglandins (Schopfer et al., 2005; Shiraki et al., 2005), whereas PPAR-δ and PPAR-α have overlapping specificities for long-chain unsaturated fatty acids (Forman et al., 1997; Chawla et al., 2003; Hostetler et al., 2005). Upon binding their

S.E. Dunn's present address is Dept. of Immunology, the University Health Network, University of Toronto, and Women's College Research Institute, Toronto, ON M5G 2M1, Canada.

The Rockefeller University Press $30.00
J. Exp. Med. Vol. 207 No. 8 1599-1608
www.jem.org/cgi/doi/10.1084/jem.20091663

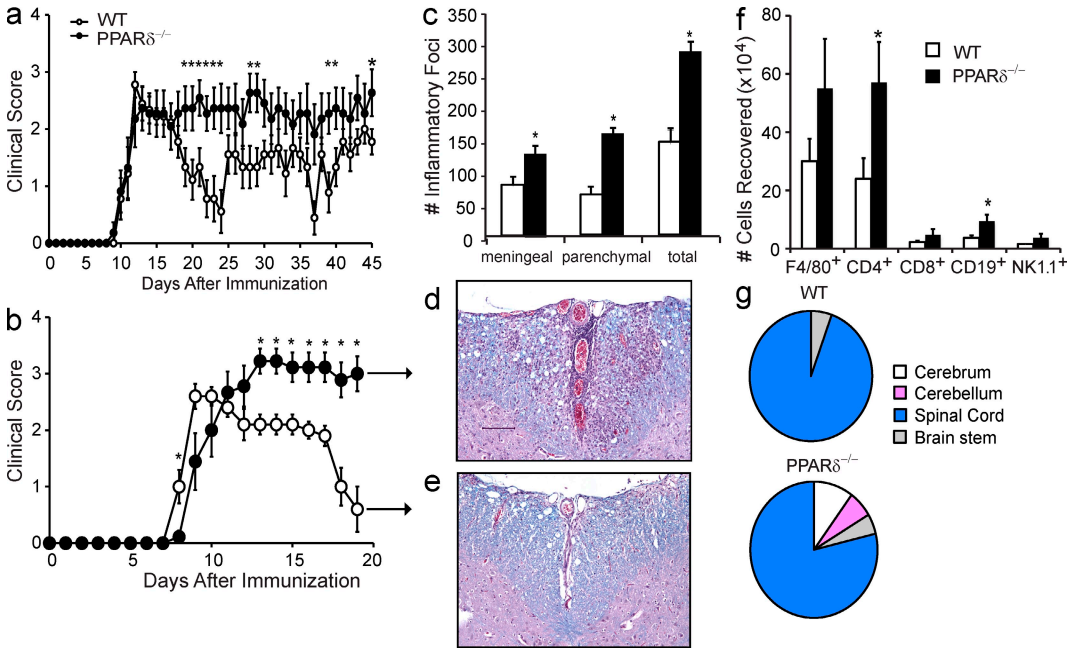

Figure 1. PPAR-δ$^{-/-}$ mice develop hyperacute EAE. EAE was induced in WT or PPAR-δ$^{-/-}$ female (a) or male (b–e) mice (n = 8–10/group). (a and b) Mean ± SEM clinical scores of mice at various times after immunization. Results are representative of two to three experiments. (c–e) Paraffin sections of spinal cord and brain were prepared from PPAR-δ$^{-/-}$ and WT mice at the time of first remission and were stained with H&E and luxol fast blue. d and e show representative sections (bar, 50 µM); c shows the mean + SEM number of inflammatory foci; g shows the regional distribution of parenchymal lesions. (f) Mononuclear cells were isolated from spinal cords of WT or PPAR-δ$^{-/-}$ mice (n = 3/group) at 4 d after the onset of clinical signs, and then they were pooled and counted. Cells were stained with antibodies specific for cell surface markers as indicated and the percentage of each subset in the live CD45$^+$ gate is shown. Values are mean + SEM numbers from four experiments. *, significantly different from WT.

ligands, PPARs in complex with 9-cis retinoic acid receptor (RXR) either activate or repress gene transcription. PPAR/RXR heterodimers transactivate expression of a wide array of genes involved in glucose and lipid metabolism by binding to PPAR-responsive elements in gene promoter regions (Straus and Glass, 2007). In immune cells, PPARs have a second function of negative regulation of AP-1 and NF-κB–dependent transcriptional activity, a mechanism which has been termed ligand-dependent transrepression (Straus and Glass, 2007).

PPARs are also activated by several synthetic drugs that are currently prescribed or are in clinical trials for the treatment of type II diabetes and dyslipidemia (thiazolidinediones for PPAR-γ, fibrates for PPAR-α, and GW0742 and GW501516 for PPAR-δ; Straus and Glass, 2007). Treatment of mice with these drugs ameliorates EAE (Feinstein et al., 2002; Lovett-Racke et al., 2004; Polak et al., 2005). The PPAR-γ agonist pioglitazone suppresses EAE by inhibiting the T cell production of IL-17A (Klotz et al., 2009) and the production of IL-12 and IL-23 by peripheral and CNS-resident myeloid cells (Storer et al., 2005). In contrast, PPAR-α appears to inhibit inflammation by shifting Th responses from Th1 to Th2 (Jones et al., 2003; Dunn et al., 2007; Gocke et al., 2009). How the PPAR-δ agonist GW0742 functions to attenuate EAE is not clear. The role of endogenously activated PPAR-δ in the control of CNS inflammation is also unknown.

In this paper, we show that PPAR-δ$^{-/-}$ mice exhibit enhanced Th cell expansion and cytokine production during EAE, as compared with WT mice, resulting in the enhanced accumulation of IFN-γ$^+$/IL-17A$^-$ and IFN-γ$^+$/IL-17A$^+$ CD4$^+$ cells in the spinal cord and more severe demyelination. Moreover, we found that the PPAR-δ ligand GW0742 inhibits the production of IFN-γ and IL-12 family members in both mouse and human immune cells. Together, these findings suggest that PPAR-δ serves as an important molecular brake for the control of CNS autoimmune inflammation.

RESULTS AND DISCUSSION

PPAR-δ limits the development of CNS inflammation during EAE

To investigate the role of endogenously activated PPAR-δ in CNS autoimmunity, we compared the clinical course of EAE in WT versus PPAR-δ$^{-/-}$ mice. Upon immunization with myelin oligodendrocyte glycoprotein (MOG) p35-55 in CFA, WT mice developed classical relapsing-remitting EAE (Fig. 1, a and b). In comparison, PPAR-δ$^{-/-}$ mice exhibited a more severe course of classical EAE, characterized by persistent hindlimb weakness (Fig. 1, a and b). Indeed, one of the main clinical features that distinguished WT and PPAR-δ$^{-/-}$ mice was that a lower frequency of mice in the PPAR-δ$^{-/-}$ group fully recovered to score 0 after the initial acute phase (Table I). This phenotype was observed in PPAR-δ$^{-/-}$ mice of both

Table I. Clinical features of EAE in male and female WT and PPAR-$\delta^{-/-}$ mice.

Clinical feautres	WT male	PPAR-$\delta^{-/-}$ male	WT female	PPAR-$\delta^{-/-}$ female
Maximum score				
Experiment 1	2.9 (0.5)	2.9 (0.2)	2.4 (0.3)	3.3 (0.6)
Experiment 2	2.9 (0.1)	2.9 (0.2)	3.3 (0.2)	3.3 (0.3)
Death from disease				
Experiment 1	1/9	0/7	0/9	2/6
Experiment 2	0/10	2/9	0/9	1/11
Incidence				
Experiment 1	8/9	7/7	9/9	6/6
Experiment 2	10/10	9/9	9/9	11/11
Day of onset				
Experiment 1	12.4 (0.5)	13.6 (1.0)	14.6 (1.4)	12.3 (0.4)
Experiment 2	8.3 (0.1)	10.9 (0.8)[a]	11.0 (0.3)	11.4 (0.8)
Number of mice remitting to score 0				
Experiment 1	7/7 (100%)	2/7 (28%)	9/9 (100%)	3/6 (50%)
Experiment 2	8/10 (80%)	1/9 (11%)	8/9 (89%)	6/11 (54%)

Values are means + SEM.
[a]Significant difference from sex-matched WT counterpart

sexes (Fig. 1, a and b) but appeared more prominently in males (Table I). Thus, males were used for subsequent experiments.

To gain insight into why EAE failed to remit in PPAR-$\delta^{-/-}$ mice, we sacrificed male WT and PPAR-$\delta^{-/-}$ mice together at the time when WT mice displayed the first improvement of clinical signs and conducted a histological analysis of the brain and spinal cord. As compared with WT mice, PPAR-$\delta^{-/-}$ mice displayed more inflammatory foci in the CNS (Fig. 1, c and d vs. e). The majority of parenchymal lesions were detected in the spinal cord in both groups; however, only in PPAR-$\delta^{-/-}$ mice were there lesions in the cerebrum and cerebellum (Fig. 1 g). As compared with the WT group, PPAR-$\delta^{-/-}$ mice also exhibited higher vacuolation/demyelination scores (mean ± SEM = 2.4 ± 0.4 in PPAR-$\delta^{-/-}$ vs. 1.2 ± 0.2 in WT, P = 0.04). Consistent with histological findings, a higher number of $CD4^+$ and $CD19^+$ cells were recovered from spinal cords of PPAR-$\delta^{-/-}$ versus WT mice during the acute phase of EAE (Fig. 1 f). Together, these results indicate that the more severe EAE that developed in PPAR-$\delta^{-/-}$ mice was the result of immune-mediated myelin and axon damage.

PPAR-δ inhibits Th1 and Th17 autoimmunity in the periphery and CNS

Because Th1 and Th17 cells can initiate and perpetuate the CNS inflammatory cascade in EAE (Diveu et al., 2008), we next examined the cytokine production by CNS-infiltrating $CD4^+$ cells during this disease. Mononuclear cells were isolated from spinal cords of WT and PPAR-$\delta^{-/-}$ mice at 4 d after the onset of clinical signs, and the production of IFN-γ and IL-17A by $CD4^+$ cells was determined by intracellular cytokine staining. This analysis revealed the presence of a higher number (Fig. 2 a) and frequency (Fig. 2 b) of IFN-γ–producing $CD4^+$ cells in spinal cords of PPAR-$\delta^{-/-}$ versus WT mice. Although we did not detect a difference in the number or frequency of IL-17A–producing cells between these two groups (Fig. 2, a and b), we did observe a trend for higher amounts of $CD4^+$ cells that coproduced both IFN-γ and IL-17A in PPAR-$\delta^{-/-}$ spinal cords (629 ± 167 in PPAR-$\delta^{-/-}$ vs. 181 ± 49 in WT, P = 0.06, n = 3 experiments; Fig. 2 c). Recent studies suggest that this Th subset is expanded by IL-23 and is highly pathogenic in the acute phase of EAE (Axtell et al., 2006; Kebir et al., 2009).

Next, we investigated whether MOG p35-55–reactive Th1 cells also underwent preferential expansion in the periphery of PPAR-$\delta^{-/-}$ mice during EAE. We harvested spleens from WT and PPAR-$\delta^{-/-}$ mice at 8 d after immunization and examined the recall proliferation and cytokine production in response to MOG p35-55 stimulation. Consistent with spinal cord findings, we found that splenocytes from PPAR-$\delta^{-/-}$ mice produced higher levels of IFN-γ, IL-17A, and TNF in response to peptide stimulation as compared with WT counterparts (Fig. 2 d). We also detected higher frequency of IFN-γ^+ IL-$17A^+CD4^+$ cells in PPAR-$\delta^{-/-}$ versus WT splenocytes by intracellular cytokine analysis (6.6 ± 1.5 in PPAR-$\delta^{-/-}$ vs. 3.0 ± 1.3 in WT, P = 0.02, n = 4 experiments). In addition, PPAR-$\delta^{-/-}$ MOG p35-55–reactive splenocytes proliferated more robustly than WT cells (Fig. 2 e). In contrast, the serum titers of MOG p35-55–specific IgM or IgG were not different between WT and PPAR-$\delta^{-/-}$ during EAE (Fig. 2 f). Thus, the more severe CNS inflammatory response in PPAR-$\delta^{-/-}$ mice correlated more with the enhanced expansion and CNS infiltration of IFN-γ– and IL-17A–producing $CD4^+$ cells.

PPAR-δ limits $CD4^+$ cell expansion and effector cytokine production

To determine whether the enhanced T cell autoimmunity in PPAR-$\delta^{-/-}$ mice was a result of intrinsic differences in $CD4^+$ cells, we contrasted the cytokine profiles of WT and PPAR-$\delta^{-/-}$ naive ($CD62L^+$) $CD4^+$ cells in response to ex vivo stimulation

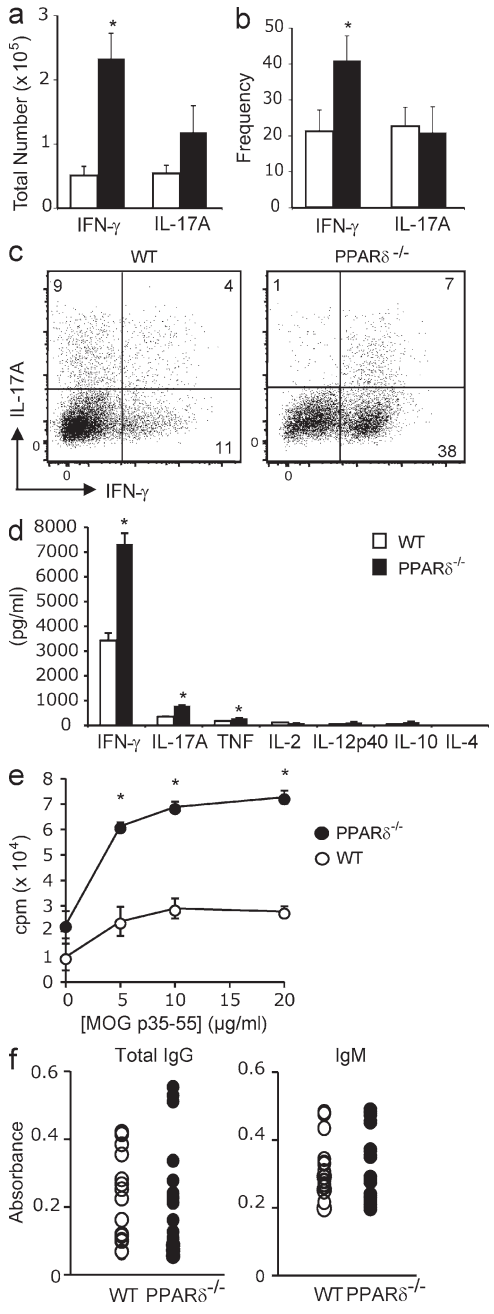

Figure 2. PPAR-δ$^{-/-}$ mice exhibit higher Th cytokine production during EAE. (a and b) Mononuclear cells were isolated from spinal cords of WT or PPAR-δ$^{-/-}$ mice at 4 d after the onset of clinical signs, and then they were pooled (n = 3/group) and processed for intracellular cytokine staining. The number (a) and frequency (b) of CD4$^+$ mononuclear cells that had intracellular accumulation of IFN-γ (IFN-γ$^+$IL-17A$^-$ and IFN-γ$^+$ IL-17A$^+$) or IL-17A (IL-17A$^+$ IFN-γ$^+$ and IL-17A$^+$ IFN-γ$^-$) are shown. (c) Representative FACs plot of IFN-γ and IL-17A staining in CD4$^+$ gate. (d and e) Splenocytes from male age-matched WT or PPAR-δ$^{-/-}$ mice were harvested at 8 d after immunization and were stimulated ex vivo with MOG p35-55. Cytokines (d) were measured in culture supernatants using ELISA. Proliferation (48 h; e) was measured by [^{3}H]-thymidine incorporation assay. Values are means + SEM of triplicate culture wells. Data in a–e are representative of three experiments. (f) Serum was collected from WT and PPAR-δ$^{-/-}$ mice during EAE. Titers of MOG p35-55–specific IgM and total IgG were determined by ELISA. Values are absorbance measurements of individual mice from two experiments that contained n = 5 and n = 11 mice/group. *, significantly different from WT.

with anti-CD3 and anti-CD28. We found that a higher proportion of naive PPAR-δ$^{-/-}$CD4$^+$ T cells than WT CD4$^+$ cells differentiated to become cytokine-producing cells in response to stimulation (Fig. 3, a and b). IFN-γ$^+$IL-17A$^-$ cells were detected at a higher frequency in cultures of PPAR-δ$^{-/-}$ versus WT cells under Th0 conditions (Fig. 3 a), whereas both IFN-γ$^-$IL-17A$^+$ and IFN-γ$^+$IL-17A$^+$ coproducing subsets were more prominent in PPAR-δ$^{-/-}$ cultures after activation under Th17-skewing conditions (Fig. 3 b). Higher production of IFN-γ and IL-17A by PPAR-δ$^{-/-}$CD4$^+$ cells was also detected at the protein level by ELISA (Fig. 3, c and d) and at the mRNA level via real-time PCR (Fig. 3, e and f). The enhanced cytokine production by PPAR-δ$^{-/-}$ CD4$^+$ cells was not limited to IFN-γ and IL-17A, as IL-2 and IL-10 were also elevated in PPAR-δ$^{-/-}$ cultures (Fig. 3, c and d). These results indicate that the enhanced Th cytokine production and dual IFN-γ/IL-17A production that we observed in PPAR-δ$^{-/-}$ mice was in part a result of intrinsic differences in CD4$^+$ cells.

Because related PPAR family members inhibit RORγT and T-bet expression (Jones et al., 2003; Klotz et al., 2009), we contrasted the mRNA levels of these transcription factors in PPAR-δ$^{-/-}$ versus WT CD4$^+$ cells. Although RORγT expression was not different between these two groups, T-bet transcripts were markedly enhanced in PPAR-δ$^{-/-}$ as compared with WT CD4$^+$ cells at 48 h after stimulation (Fig. 3 h). Given results that T-bet supports expansion of both Th1 and Th17 cells and is more highly expressed in double-positive (IFN-γ$^+$IL-17$^+$) versus IFN-γ single-positive CD4$^+$ cells (Yang et al., 2009), the higher levels of this transcription factor may explain the propensity of PPAR-δ$^{-/-}$CD4$^+$ cells for dual IFN-γ/IL-17A production. Nevertheless, our finding that T-bet mRNA expression trailed the peak in IFN-γ mRNA indicates that it is not the sole cause of enhanced cytokine production by PPAR-δ$^{-/-}$CD4$^+$ cells.

Consistent with the reported role for PPAR-δ in regulating cell growth (Peters and Gonzalez, 2009), we also observed that PPAR-δ$^{-/-}$CD4$^+$ cells proliferated to a greater extent than WT CD4$^+$ cells in response to anti-CD3 and anti-CD28 stimulation (Fig. 4 a). Interestingly, spleens taken directly from nonimmunized PPAR-δ$^{-/-}$ mice exhibited a higher frequency of CD4$^+$ cells that displayed a memory (CD44^{high}CD62L$^-$) or activated (CD69$^+$) CD4$^+$ phenotype (Fig. 4, c and d). In contrast, we did not detect differences in the proliferation rates of WT and PPAR-δ$^{-/-}$ B cells (Fig. 4 b). Collectively with cytokine findings, these results indicate that PPAR-δ negatively regulates the activation state and effector function of CD4$^+$ cells.

Finally, to confirm that a defect of PPAR-δ in the T cell compartment was causal to the hyperexpansion of MOG p35-55–reactive CD4$^+$ cells that we observed in

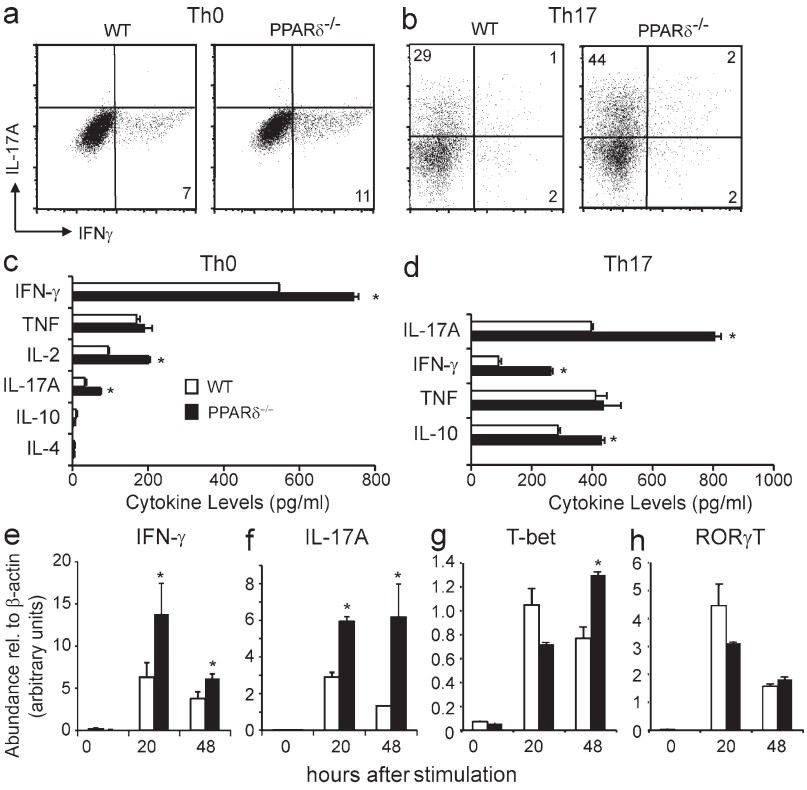

Figure 3. PPAR-δ limits cytokine production by CD4+ cells. (a–c) Naive CD4+ cells were isolated from the spleens of WT or PPAR-$\delta^{-/-}$ mice and stimulated with anti-CD3 and anti-CD28 under Th0-skewing (a, c, e, and g) or Th17-skewing (b, d, f, and h), conditions. After 4 d of culture, CD4+ cells were processed for intracellular cytokine staining. (a and b) Representative FACs plots of events in the CD4+ gate. (c and d) Cytokine levels in culture supernatants after 48 h of culture under Th0-skewing (c) or Th17-skewing (d) conditions. (e–h) mRNA levels of IFN-γ and T-bet (Th0 conditions) or IL-17A and RORγt (Th17 conditions; relative to β-actin mRNAs) were determined using real-time PCR. *, significantly different from WT. Values are means + SEM of triplicate cultures (c and d) or triplicate reactions (e–h). Data are representative of two to five experiments.

PPAR-$\delta^{-/-}$ during EAE, we made chimeras by reconstituting B6.Rag1$^{-/-}$ mice with either WT or PPAR-$\delta^{-/-}$ CD4+ T cells. We then immunized these mice with MOG p35-55/CFA, and examined the expansion and encephalitogenicity of transferred CD4+ cells. Splenocytes from the Rag1$^{-/-}$ mice reconstituted with the PPAR-$\delta^{-/-}$CD4+ cells exhibited higher IFN-γ and IL-17A production as compared with those transferred with WT CD4+ cells (Fig. S1 a). Although only a small fraction (~25%) of mice in both groups succumbed to EAE, more WT B6.Rag1$^{-/-}$ than PPAR-$\delta^{-/-}$B6.Rag1$^{-/-}$ mice developed a relapsing-remitting course (four of four of WT vs. one of four PPAR-$\delta^{-/-}$B6.Rag1$^{-/-}$; Fig. S1 b). These results indicate that PPAR-δ acts in the CD4+ cell compartment to limit expansion of Th1 and Th17 cells and to dampen CNS inflammation during EAE.

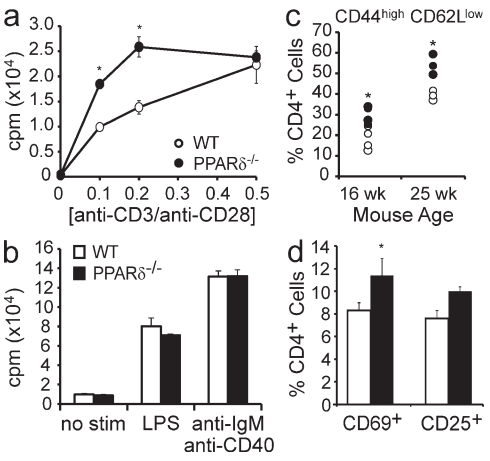

Figure 4. CD4+ T cells from PPAR-$\delta^{-/-}$ mice are hyperresponsive. Naive CD4+ (a) or CD19+ (b) cells were isolated from the spleens of WT or PPAR-$\delta^{-/-}$ mice and were stimulated as indicated. Proliferation of these cells was measured using a [^{3}H]-thymidine incorporation assay. Values are means + SEM of triplicate cultures. (c and d) Splenocytes were harvested from nonimmunized WT or PPAR-$\delta^{-/-}$ mice. The frequency of CD4+ cells that displayed a memory (CD44^{high} and CD62L^{low}; c) or activated (CD69+ or CD25+; d) phenotype in each group was determined. In d, values represent mean + SEM frequencies of n = 3–4 mice/group. Data in a–d are representative of two experiments. *, significantly different from WT.

PPAR-δ inhibits expression of IL-12 family cytokines

Both IFN-γ+/IL-17A− and IFN-γ+/IL-17A+ CD4+ cells were detected in spinal cords of PPAR-$\delta^{-/-}$ mice during EAE. The former Th subset is induced by IL-12, whereas the latter subset is expanded by IL-23 (Awasthi et al., 2009; McGeachy et al., 2009). Given results that the related nuclear receptor PPAR-γ negatively regulates IL-12p40 (common to IL-12 and IL-23; Storer et al., 2005), we investigated whether myeloid cells from PPAR-$\delta^{-/-}$ mice have a higher propensity to produce this or other IL-12 family cytokines. Indeed, we found that splenic cd11b+ cells and peritoneal macrophages from PPAR-$\delta^{-/-}$ mice produced higher levels of IL-12p40 as compared with WT counterparts (Fig. 5, a and b). A small amount of IL-12p70 (p35/p40 heterodimer) was also detected in supernatants of PPAR-$\delta^{-/-}$ cells at levels that were higher than those observed in WT. In contrast, we did not detect a consistent difference in the production of other cytokines between these groups. Similar to ELISA findings, we also observed that the mRNA expression of the IL-12 family members IL-12p40, IL-23p19, and IL-12p35 were markedly elevated in PPAR-$\delta^{-/-}$ versus WT splenic cd11b+ cells after LPS stimulation (Fig. 5 c). Because myeloid cells drive the expansion of Th cells in the CNS during EAE (Bailey et al., 2007),

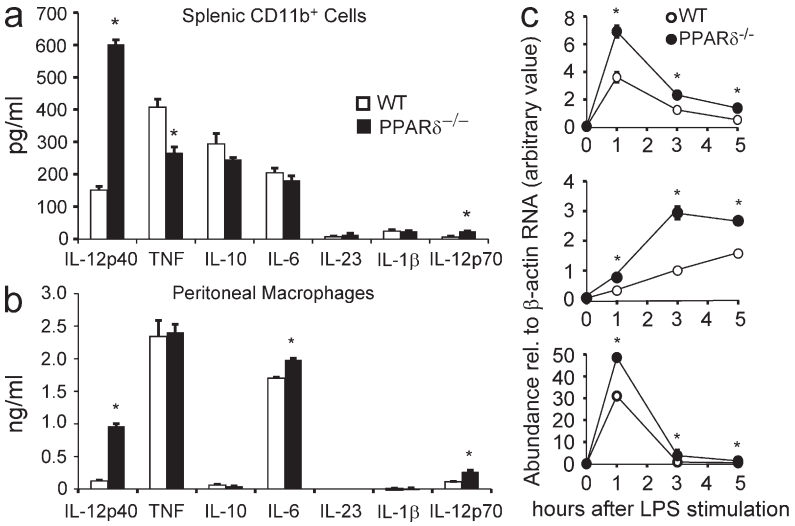

Figure 5. PPAR-δ negatively regulates expression of IL-12 family cytokines. Splenic CD11b$^+$ cells (a and c) or peritoneal macrophages (b) were isolated from adult age-matched WT and PPAR-$\delta^{-/-}$ mice and were cultured with 10 ng/ml LPS. (a and b) Supernatants were collected at 24 h for cytokine measurement by ELISA. (c) Cells were harvested at 0, 1, 3, or 5 h after stimulation for collection of RNA for real-time PCR measurement of p40, p35, or p19 mRNA expression (relative to β-actin). Values represent mean + SEM of triplicate cultures (a and b) or reactions (c). *, significantly different from WT. Results are representative of three experiments.

this finding that PPAR-$\delta^{-/-}$ macrophages have a higher propensity to produce IL-12 family cytokines may further explain the preferential accumulation of IFN-γ^+/IL-17A$^-$ and IFN-γ^+/IL-17A$^+$ CD4$^+$ cells in the CNS of PPAR-$\delta^{-/-}$ mice during this disease.

PPAR-δ suppresses IFN-γ and IL-12 production in a ligand-dependent manner

PPAR-δ is reported to have both ligand-dependent and -independent actions in vivo (Straus and Glass, 2007). To test how the ligand dependency of PPAR-δ affects Th cell production, we stimulated WT or PPAR-$\delta^{-/-}$ CD4$^+$ T cells with anti-CD3 and anti-CD28 in the presence or absence of the specific PPAR-δ agonist GW0742. We used up to 1 μM of this drug because preliminary experiments indicated that GW0742 has off-target effects at ≥1-μM concentrations. These initial experiments revealed that GW0742 triggered an increase in Th1 cytokine production by WT CD4$^+$ cells (Fig. 6 a). These results were unexpected given our results in PPAR-$\delta^{-/-}$ mice; however, they were consistent with previous results of GW0742 on Th1 cytokine production during EAE (Polak et al., 2005).

Because bovine serum is a potential source of several endogenous PPAR-δ ligands, we posited that the failure of GW0742 to dampen Th1 cytokine production was because PPAR-δ was already saturated with a serum-derived ligand. To test this possibility, we repeated the experiment using serum-free X-vivo 20 media. Under these conditions, GW0742 had the expected effect of decreasing the production of IFN-γ by WT but not by PPAR-$\delta^{-/-}$ CD4$^+$ cells (Fig. 6, b–d).

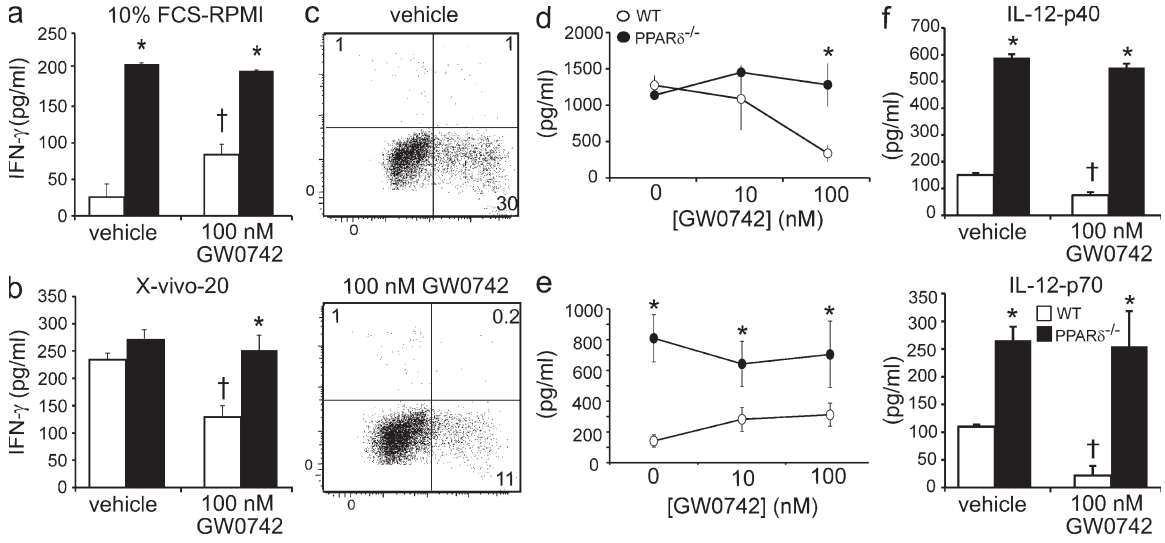

Figure 6. GW0742 suppresses IFN-γ and IL-12 family cytokines in a PPAR-δ–dependent manner. CD4$^+$ cells (a–e) or peritoneal macrophages (f) were stimulated in the presence of 100 nM GW0742 or vehicle of equal volume. Cells were cultured in complete RPMI (a) or X-vivo 20 serum-free media (b–f). CD4$^+$ cells were stimulated with anti-CD3 under Th0-skewing (a–d) or Th17-skewing (e) conditions, whereas peritoneal macrophages were stimulated with LPS. Cytokine production was measured after 24 or 48 h of culture by ELISA and intracellular staining was conducted after 4 d of culture as in Fig. 3. Values represent means + SEM of triplicate cultures. *, significantly different from WT. †, significantly different from vehicle counterpart. Results are representative of three experiments.

Table II. Cytokine production by human PBMCs treated with 100 nM GW0742

Stimulus	Donor 1		Donor 2		Donor 3	
	Vehicle	GW0742	Vehicle	GW0742	Vehicle	GW0742
α-CD3 and α-CD28						
IL-2	122 (7)	160 (8)[a]	178 (5)	200 (11)	92 (11)	93 (4)
IL-17A	21 (2)	25 (1)	14 (1)	16 (5)	16 (1)	14 (1)
TNF	140 (12)	113 (13)	491 (17)	400 (88)	1,019 (50)	1,178 (50)
IFN-γ	1,231 (213)	716 (33)[a]	4,205 (129)	3,125 (271)[a]	3,087 (111)	2,547 (97)[a]
LPS						
IL-12p40	7,160 (152)	4,541 (162)[a]	5,497 (264)	3,203 (328)[a]	8,881 (367)	5,562 (318)[a]
IL-23	3,581 (54)	2,507 (109)[a]	2,262 (41)	1,450 (50)[a]	3,775 (136)	2,508 (124)[a]
IL-12p70	322 (38)	275 (36)	1,486 (145)	991 (85) [a]	1,195 (187)	1,335 (157)

Values are means + SEM of cytokine levels (pg/ml) in triplicate cultures.
[a]Significant difference from vehicle control cultures using a Student's *t* test (P = 0.05, two-tailed).

Similarly, GW0742 suppressed the production of IL-12p40 in a PPAR-δ–specific fashion by macrophages (Fig. 6 f). Interestingly, treatment with GW0742 did not lower the production of IL-17A by WT T cells as detected by ELISA (Fig. 6 e), indicating that the enhanced production of IL-17A by PPAR-$\delta^{-/-}$ $CD4^+$ cells was likely related to general effects of PPAR-δ on T cell expansion.

Transcriptional regulation of IFN-γ is complex, as it is dictated by the interaction of functional genomic elements acting as far as 50 kb from this gene (Aune et al., 2009). Comparatively, the LPS-induced transcription of IL-12p40 is more straightforward, as it involves the binding of well characterized transcription factors (i.e., NF-κB) to genomic elements in the proximal promoter of this gene (Murphy et al., 1995). We thus pursued studies of the IL-12p40 promoter to gain insight into the mechanism of ligand inhibition of cytokine production. We observed that GW0742 repressed IL-12p40 promoter activity in RAW264.7 cells that were transfected with an IL-12p40/luciferase reporter construct (Fig. S2). This ligand effect was dose and PPAR-δ dependent (Fig. S2). This result indicates that PPAR-δ works via a mechanism of transcriptional repression to regulate IL-12p40 gene expression.

PPAR-δ inhibits the production of IFN-γ and IL-12 family cytokines by PBMCs

Given that GW0742 is a ligand agonist of both mouse and human PPAR-δ, we investigated whether this drug modulates cytokine production by human immune cells. We obtained PBMCs from three male healthy donors and then cultured these cells in serum-free media containing either 100 nM GW0742 or vehicle control in the presence of either anti-CD3 and anti-CD28 or LPS. Similar to findings in the mouse system, we found that 100 nM GW0742 selectively reduced the production of IFN-γ by PBMCs in response to anti-CD3 and anti-CD28, and it blunted the LPS induction of IL-12p40 and IL-23 (Table II). These effects were observed in three of three donors.

Concluding remarks

This study provides new evidence that PPAR-δ is an important negative regulator of CNS autoimmune inflammation. We found that mice deficient in this nuclear receptor exhibit a severe course of EAE characterized by a preferential accumulation of IFN-γ^+IL-17A^- and IFN-γ^+IL-17A^+ $CD4^+$ subsets in the CNS. This appeared to occur as a result of several immune aberrations that included a hyperresponsive $CD4^+$ T cell population and higher IL-12 family cytokine production by myeloid cells. We also found that the PPAR-δ ligand GW0742 inhibits the production of IFN-γ and IL-12p40 by both mouse and human immune cells, indicating that these immune regulatory effects of PPAR-δ are ligand dependent and conserved between mouse and man. Taken in this light, our observation of immune phenotypic differences between WT and PPAR-$\delta^{-/-}$ mice, in the absence of treatment with synthetic ligands, suggests that that PPAR-δ likely binds an endogenous ligand to mediate its anti-inflammatory effects in vivo. Future studies will investigate the nature of these ligands as well as the molecular mechanism of inhibition of IFN-γ and IL-12 family cytokines by PPAR-δ.

MATERIALS AND METHODS

Mice and EAE induction. Mice that have targeted disruption of the last exon of PPAR-β/δ gene containing the ligand-binding and RXR heterodimerization domains have been described previously (Peters et al., 2000). Homozygote mice express a truncated unstable PPAR-δ transcript, resulting in no detectable PPAR-δ protein (Peters et al., 2000). These mice, herein referred to as PPAR-$\delta^{-/-}$ mice, were originally on an outbred (129 × $B6_{Fl}$) background and were crossed six generations to C57BL/6. PPAR-$\delta^{-/-}$ pups could not be generated past the sixth generation. Thus, WT and mutant colonies were established from the sixth generation. Genotyping of PPAR-$\delta^{-/-}$ mice and WT counterparts was performed by amplifying a portion of the ligand-binding domain of PPAR-δ or the neo cassette insert of the mutant allele from tail DNA (cycling conditions: 1 min at 94°C, 1 min at 60°C, and 1 min at 72°C). Primer sequences were: PPAR-δ forward, 5′-CAGGATGTCCTTCCACAGAGACAG-3′; PPAR-δ reverse, 5′-TTAGCCACTGCATCATCTGGG-3′; and neo cassette, 5′-GCAATCCATCTTGTTCAATGGC-3′.

EAE was induced in PPAR-$\delta^{-/-}$ mice (8–12 wk of age) and age-matched WT counterparts via subcutaneous immunization with 100 μg MOG p35-55 in an emulsion with CFA (Dunn et al., 2007). Mice were also

injected intravenously with 50 ng *Bordetella* pertussis toxin (BD) at the time of, and 2 d after, immunization. Mice (n = 8–10/group) were examined daily for clinical signs of EAE and were scored on a five point scale: 0, no clinical disease; 1, limp tail; 2, hindlimb weakness; 3, complete hindlimb paralysis; 4, hindlimb paralysis plus some forelimb paralysis; and 5, moribund or dead. We found that clinical phenotype of PPAR-$\delta^{-/-}$ mice was pronounced in males. Thus, we conducted all subsequent experiments in male mice. Animal protocols were approved by the Division of Comparative Medicine at Stanford University and animals were maintained in accordance with the guidelines of the National Institutes of Health.

MOG p35-55–specific Th responses. At 8 d after immunization (in EAE experiments), spleens were recovered from nonsick immunized mice (n = 3 mice/group) and were dissociated into a single cell suspension. Red blood cells were lysed and splenocytes were cultured in 96-well plates (0.5×10^6 cells/well) with 0–25 μg/ml MOG p35-55 in complete RPMI (RPMI 1640 supplemented with 2 mM L-glutamine, 1 mM sodium pyruvate, 0.1 mM nonessential amino acids, 100 U/ml penicillin, 0.1 mg/ml streptomycin, 0.5 μM 2-mercaptoethanol, and 10% fetal calf serum). Culture supernatants were harvested at 24–72 h after stimulation for cytokine measurement by ELISA (BD, R&D Systems, and eBioscience kits).

Rag transfer experiments. $CD4^+$ cells were isolated from spleens of male PPAR-$\delta^{-/-}$ mice (n = 10 mice/group), pooled together, and $7–10 \times 10^6$ of these cells were injected intravenously into B6.Rag1$^{-/-}$ recipients (The Jackson Laboratory). B6.Rag1$^{-/-}$ transferred with WT $CD4^+$ cells served as controls. EAE was induced in these mice at 48 h after transfer as described previously (Dunn et al., 2007). Approximately 25% of mice in each group developed clinical signs. Nonsick mice were used to investigate the role for T cell–expressed PPAR-δ in the regulation of MOG p35-55 splenocyte responses.

MOG p35-55–specific IgG and IgM responses. Mice were bled at day 28 of disease. MOG p35-55–specific antibodies were detected in the sera of mice using an ELISA assay. In brief, plates were coated overnight at 4°C with 10 μg/ml MOG p35-55 peptide and then blocked with 3% fetal calf serum before serial probing with sera (1:100 diluted, 2 h), followed by a 1-h incubation with horseradish peroxidase–conjugated goat anti–mouse IgG or IgM (SouthernBiotech). Plates were washed three times with 0.5% PBS containing Tween 20 between each step. Horseradish peroxidase conjugates were detected using tetramethylbenzidine substrate. Absorbances were measured at 450 nm and background levels were subtracted.

Histopathology. Brains and spinal cords were dissected from male mice (n = 5/group), fixed in 10% formalin in PBS, and embedded in a single paraffin block. 6–10-μm-thick sections were stained with hematoxylin and eosin and luxol fast blue. The number of meningeal and parenchymal inflammatory foci was counted in brain and spinal cord sections by a trained neuropathologist who was blinded to the clinical and treatment status of the animal. A demyelination/vacuolation score was also assigned to each specimen that ranged in severity from 0 (absence of demyelination/vacuolation) to 4 (severe demyelination/vacuolation).

Isolation of CNS mononuclear cells. CNS mononuclear cells were isolated from mice (n = 3 mice/group) at 5 d after the onset of EAE. Mice were anaesthetized (80–100 mg/kg ketamine hydrochloride: 10 mg/kg xylazine) and perfused with PBS containing 5 U/ml heparin. Spinal cords were pooled together (n = 3), scissor minced into Hank's buffered saline, and then digested for 45 min at 37°C with 300 U/ml Clostridial collagenase type IV (Roche) and 1 mg/ml DNase (Sigma-Aldrich). After digestion, the spinal cord tissue was dissociated through a 70-μm sieve. This filtrate was centrifuged and the pellet containing the mononuclear cells was resuspended in 30% Percoll (GE Healthcare). This suspension was underlaid with 70% Percoll and centrifuged at 1,800 rpm for 10 min. Mononuclear cells were collected from the 30/70% interface, washed twice, and suspended in complete RPMI.

FACS staining of cell subsets in the spleen and CNS. FACs staining of splenocyte and CNS mononuclear cells was done using BD antibodies and protocols unless otherwise noted. Antibodies directed against the following mouse cell surface antigens were used: CD4, CD8, CD19, CD11b, CD11c, CD44, CD45, CD62L, and F4/80 antigen (AbD Serotec). Intracellular staining of mouse FoxP3 was performed using a kit from eBioscience. For intracellular cytokine staining, cells were stimulated for 4 h with 10 ng/ml PMA and 750 nM ionomycin in the presence of GolgiStop to cause intracellular accumulation of cytokines. Cells were then stained with anti-CD4 and fixable aqua live/dead dye (Invitrogen) before fixation, permeabilization, and intracellular staining for mouse anti–IFN-γ and IL-17A. Data were acquired using a Flasher II cell sorter (BD) or LSRII analyzer and the frequency of $CD45^+/CD4^+$ cells expressing IFN-γ and IL-17 was analyzed using FlowJo software (Tree Star, Inc.).

Culture of isolated myeloid and Th cell populations. $CD11b^+$ or $CD19^+$ cells were isolated by positive selection and $CD4^+$ cells by negative selection using reagents (Miltenyi Biotec). The naive $CD4^+$ fraction was further fractionated using $CD62L^+$ magnetic beads provided in the naive mouse $CD4^+$ isolation kit (Miltenyi Biotec). Peritoneal macrophages were harvested from the peritoneum of mice at 3 d after i.p. injection with thioglycollate. These cells were washed, plated in flat-bottom plates (2×10^5/well), and allowed to rest overnight (with vehicle or GW0742) before stimulation with LPS. All cells were resuspended in complete RPMI or in X-vivo 20 serum-free media (Lonza; serum-free media also contained 2 mM L-glutamine, 1 mM sodium pyruvate, 0.1 mM nonessential amino acids, 100 U/ml penicillin, 0.1 mg/ml streptomycin, and 0.5 μM 2-mercaptoethanol). T cells were cultured with 0.1–0.5 μg/ml of plate-bound anti-CD3 (clone 145-2C11; BD) and α-CD28 (clone 37.51; BD) under Th0-skewing conditions (no added cytokines) or Th17-skewing conditions (20 ng/ml of mouse recombinant IL-6, 3 ng/ml of human recombinant TGF-β, and 10 μg/ml of anti–IFN-γ (XMG1.2). Peritoneal macrophages or splenic $cd11b^+$ cells were cultured in flat-bottomed 96-well plates with 1–100 ng/ml LPS. Cytokines were measured in the supernatants of cultured cells at 24–72 h using commercial ELISA kits.

Proliferation. Proliferation rate of T cells and B cells was measured as described previously (Dunn et al., 2007).

Real-time PCR. RNA was extracted from naive $CD4^+$ T cells immediately after isolation or after 24 h of culture using Absolutely RNA kits (Agilent Technologies). Real-time PCR was conducted using the standard curve method, using SYBR Green reagents (QIAGEN) and the following specific primer sets: IL-12p40 forward, 5′-TCCCCATTCCTACTTCTCCCTC-3′; IL-12p40 reverse, 5′-GGAACGCACCTTTCTGGTTACA-3′; IL-12p35 forward, 5′-CACGCTACCTCCTCTTTTTG-3′; IL-12p35 reverse, 5′-CAGCAGTGCAGGAATAATGTT-3′; IL-23p19 forward, 5′-AATCTCTGCATGCTAGCCTGG-3′; IL-23p19 reverse, 5′-GATTCATATGTCCCGCTGGTG-3′; T-bet forward, 5′-AATGCCGCTGAATTGG-3′; T-bet reverse, 5′-CGTGACTGTAGTTCGGG-3′; RORγT forward, 5′-AGATTGCCCTCTACACG-3′; RORγT reverse, 5′-GGCTTGGACCACGATG-3′; β-actin forward, 5′-TGTCCCTGTATGCCTCTGGT-3′; and β-actin reverse 5′-CACGCACGATTTCCCTCTC-3′. IFN-γ and IL-17 mRNAs were measured using one-step EZ Taqman reagents and Taqman primer probe sets (Applied Biosystems). Expression was normalized to either β-actin or 18S ribosomal RNA (primers from SuperArray).

IL-12p40 promoter analysis. The RAW264.7 mouse macrophage cell line was maintained in RPMI1640 medium supplemented with 10% fetal bovine serum, 100 U/ml penicillin, and 100 μg/ml streptomycin. Cells were transfected using Lipofectamine 2000 (Invitrogen) and were cultured in 6-well plates in low-serum (0.5% FBS) media containing penicillin and streptomycin. The luciferase reporter DM-703, in which luciferase transcription is directed by a mouse IL12p40 promoter fragment extending to −703, was obtained from K.M. Murphy (Washington University School of Medicine,

St. Louis, MO; Murphy et al., 1995). The plasmid pCMV-βgal was cotransfected along with the luciferase reporter as an internal control for transfection efficiency and for the specificity of the effects observed. The plasmid pCMX-PPAR-δ was used for expression of mouse PPAR-δ (Forman et al., 1997). To determine the effect of GW0742 on promoter activity, cells were pretreated with GW0742 for 1 h before addition of LPS (final concentration, 100 ng/ml). Incubation was continued for 6 h, after which the cells were harvested for luciferase and β-galactosidase assays.

Culture of human PBMCs. PBMCs were isolated from peripheral blood of three healthy donors using Ficoll gradient. These cells were resuspended in X-vivo 15 media containing 2 mM L-glutamine, 1 mM sodium pyruvate, 0.1 mM nonessential amino acids, 100 U/ml penicillin, 0.1 mg/ml streptomycin, and 0.5 μM 2-mercaptoethanol. Either 100 nM of GW0742 or an equal volume of vehicle was added to cells, and they were plated (2×10^5/well) in flat-bottomed plates. After 2 h of vehicle or ligand treatment, Dynabeads human T cell expander (1 Dynabead for every 10 T cells; Invitrogen) or 10 ng/ml LPS was added to cells. Cytokines were measured in culture supernatants at 48 or 72 h using IFN-γ, IL-2, TNF, and IL-17A ELISA kits (eBioscience) and an IL-12p40 kit (BD).

Statistical analysis. Data are presented as means + SEM. When data were parametric (kurtosis and skewness < 2), a Student's *t* test (two-tailed) was used to detect between-group differences. When data were nonparametric, ranks were compared among groups using a Mann-Whitney *U* test. A value of $P \leq 0.05$ was considered significant.

Online supplemental material. Fig. S1 depicts the results from EAE studies using $Rag^{-/-}$ mice transferred with WT or PPAR-$\delta^{-/-}$ $CD4^+$ cells. Fig. S2 depicts the results from the IL-12p40 luciferase reporter experiment. Online supplemental material is available at http://www.jem.org/cgi/content/full/jem.20091663/DC1.

The authors thank Anne Marie Barrette and Melissa Miranda for assistance with ELISA assays and Jing Liu for assistance with transfection assays.

This work was supported by grants made available to L. Steinman (National Institutes of Health [NIH] and National Multiple Sclerosis Society [NMSS]), A. Chawla (NIH DK062386, HL076746, and DK081405 and Rita Allen Foundation), and S.E. Dunn (Multiple Sclerosis Society of Canada). R. Bhat and R. Axtell are funded by postdoctoral fellowships from the NMSS. J.C. Dugas is funded by National Eye Institute grant NIH 5 R01 EY10257-12.

The authors have no conflicting financial interests.

Submitted: 29 July 2009
Accepted: 9 June 2010

REFERENCES

Aune, T.M., P.L. Collins, and S. Chang. 2009. Epigenetics and T helper 1 differentiation. *Immunology*. 126:299–305. doi:10.1111/j.1365-2567.2008.03026.x

Awasthi, A., L. Riol-Blanco, A. Jäger, T. Korn, C. Pot, G. Galileos, E. Bettelli, V.K. Kuchroo, and M. Oukka. 2009. Cutting edge: IL-23 receptor gfp reporter mice reveal distinct populations of IL-17-producing cells. *J. Immunol.* 182:5904–5908. doi:10.4049/jimmunol.0900732

Axtell, R.C., L. Xu, S.R. Barnum, and C. Raman. 2006. CD5-CK2 binding/activation-deficient mice are resistant to experimental autoimmune encephalomyelitis: protection is associated with diminished populations of IL-17-expressing T cells in the central nervous system. *J. Immunol.* 177:8542–8549.

Bailey, S.L., B. Schreiner, E.J. McMahon, and S.D. Miller. 2007. CNS myeloid DCs presenting endogenous myelin peptides 'preferentially' polarize $CD4^+$ T(H)-17 cells in relapsing EAE. *Nat. Immunol.* 8:172–180. doi:10.1038/ni1430

Chawla, A., C.H. Lee, Y. Barak, W. He, J. Rosenfeld, D. Liao, J. Han, H. Kang, and R.M. Evans. 2003. PPARdelta is a very low-density lipoprotein sensor in macrophages. *Proc. Natl. Acad. Sci. USA*. 100:1268–1273. doi:10.1073/pnas.0337331100

Diveu, C., M.J. McGeachy, and D.J. Cua. 2008. Cytokines that regulate autoimmunity. *Curr. Opin. Immunol.* 20:663–668. doi:10.1016/j.coi.2008.09.003

Dunn, S.E., S.S. Ousman, R.A. Sobel, L. Zuniga, S.E. Baranzini, S. Youssef, A. Crowell, J. Loh, J. Oksenberg, and L. Steinman. 2007. Peroxisome proliferator–activated receptor (PPAR) α expression in T cells mediates gender differences in development of T cell–mediated autoimmunity. *J. Exp. Med.* 204:321–330. doi:10.1084/jem.20061839

Feinstein, D.L., E. Galea, V. Gavrilyuk, C.F. Brosnan, C.C. Whitacre, L. Dumitrescu-Ozimek, G.E. Landreth, H.A. Pershadsingh, G. Weinberg, and M.T. Heneka. 2002. Peroxisome proliferator-activated receptor-gamma agonists prevent experimental autoimmune encephalomyelitis. *Ann. Neurol.* 51:694–702. doi:10.1002/ana.10206

Forman, B.M., J. Chen, and R.M. Evans. 1997. Hypolipidemic drugs, polyunsaturated fatty acids, and eicosanoids are ligands for peroxisome proliferator-activated receptors alpha and delta. *Proc. Natl. Acad. Sci. USA*. 94:4312–4317. doi:10.1073/pnas.94.9.4312

Gocke, A.R., R.Z. Hussain, Y. Yang, H. Peng, J. Weiner, L.H. Ben, P.D. Drew, O. Stuve, A.E. Lovett-Racke, and M.K. Racke. 2009. Transcriptional modulation of the immune response by peroxisome proliferator-activated receptor-alpha agonists in autoimmune disease. *J. Immunol.* 182:4479–4487. doi:10.4049/jimmunol.0713927

Hostetler, H.A., A.D. Petrescu, A.B. Kier, and F. Schroeder. 2005. Peroxisome proliferator-activated receptor alpha interacts with high affinity and is conformationally responsive to endogenous ligands. *J. Biol. Chem.* 280:18667–18682. doi:10.1074/jbc.M412062200

Jones, D.C., X. Ding, T.Y. Zhang, and R.A. Daynes. 2003. Peroxisome proliferator-activated receptor alpha negatively regulates T-bet transcription through suppression of p38 mitogen-activated protein kinase activation. *J. Immunol.* 171:196–203.

Kebir, H., I. Ifergan, J.I. Alvarez, M. Bernard, J. Poirier, N. Arbour, P. Duquette, and A. Prat. 2009. Preferential recruitment of interferon-gamma-expressing T H 17 cells in multiple sclerosis. *Ann. Neurol.* 66:390–402. doi:10.1002/ana.21748

Klotz, L., S. Burgdorf, I. Dani, K. Saijo, J. Flossdorf, S. Hucke, J. Alferink, N. Nowak, N. Novak, M. Beyer, et al. 2009. The nuclear receptor PPAR gamma selectively inhibits Th17 differentiation in a T cell-intrinsic fashion and suppresses CNS autoimmunity. *J. Exp. Med.* 206:2079–2089. doi:10.1084/jem.20082771

Kroenke, M.A., T.J. Carlson, A.V. Andjelkovic, and B.M. Segal. 2008. IL-12– and IL-23–modulated T cells induce distinct types of EAE based on histology, CNS chemokine profile, and response to cytokine inhibition. *J. Exp. Med.* 205:1535–1541. doi:10.1084/jem.20080159

Langrish, C.L., Y. Chen, W.M. Blumenschein, J. Mattson, B. Basham, J.D. Sedgwick, T. McClanahan, R.A. Kastelein, and D.J. Cua. 2005. IL-23 drives a pathogenic T cell population that induces autoimmune inflammation. *J. Exp. Med.* 201:233–240. doi:10.1084/jem.20041257

Lock, C., G. Hermans, R. Pedotti, A. Brendolan, E. Schadt, H. Garren, A. Langer-Gould, S. Strober, B. Cannella, J. Allard, et al. 2002. Gene-microarray analysis of multiple sclerosis lesions yields new targets validated in autoimmune encephalomyelitis. *Nat. Med.* 8:500–508. doi:10.1038/nm0502-500

Lovett-Racke, A.E., R.Z. Hussain, S. Northrop, J. Choy, A. Rocchini, L. Matthes, J.A. Chavis, A. Diab, P.D. Drew, and M.K. Racke. 2004. Peroxisome proliferator-activated receptor alpha agonists as therapy for autoimmune disease. *J. Immunol.* 172:5790–5798.

McGeachy, M.J., Y. Chen, C.M. Tato, A. Laurence, B. Joyce-Shaikh, W.M. Blumenschein, T.K. McClanahan, J.J. O'Shea, and D.J. Cua. 2009. The interleukin 23 receptor is essential for the terminal differentiation of interleukin 17-producing effector T helper cells in vivo. *Nat. Immunol.* 10:314–324. doi:10.1038/ni.1698

Murphy, T.L., M.G. Cleveland, P. Kulesza, J. Magram, and K.M. Murphy. 1995. Regulation of interleukin 12 p40 expression through an NF-κB half-site. *Mol. Cell. Biol.* 15:5258–5267.

Peters, J.M., and F.J. Gonzalez. 2009. Sorting out the functional role(s) of peroxisome proliferator-activated receptor-β/δ (PPARbeta/δ) in cell proliferation and cancer. *Biochim. Biophys. Acta.* 1796:230–241.

Peters, J.M., S.S. Lee, W. Li, J.M. Ward, O. Gavrilova, C. Everett, M.L. Reitman, L.D. Hudson, and F.J. Gonzalez. 2000. Growth, adipose,

brain, and skin alterations resulting from targeted disruption of the mouse peroxisome proliferator-activated receptor beta(delta). *Mol. Cell. Biol.* 20:5119–5128. doi:10.1128/MCB.20.14.5119-5128.2000

Polak, P.E., S. Kalinin, C. Dello Russo, V. Gavrilyuk, A. Sharp, J.M. Peters, J. Richardson, T.M. Willson, G. Weinberg, and D.L. Feinstein. 2005. Protective effects of a peroxisome proliferator-activated receptor-beta/delta agonist in experimental autoimmune encephalomyelitis. *J. Neuroimmunol.* 168:65–75. doi:10.1016/j.jneuroim.2005.07.006

Schopfer, F.J., Y. Lin, P.R. Baker, T. Cui, M. Garcia-Barrio, J. Zhang, K. Chen, Y.E. Chen, and B.A. Freeman. 2005. Nitrolinoleic acid: an endogenous peroxisome proliferator-activated receptor gamma ligand. *Proc. Natl. Acad. Sci. USA.* 102:2340–2345. doi:10.1073/pnas.0408384102

Shiraki, T., N. Kamiya, S. Shiki, T.S. Kodama, A. Kakizuka, and H. Jingami. 2005. Alpha,beta-unsaturated ketone is a core moiety of natural ligands for covalent binding to peroxisome proliferator-activated receptor gamma. *J. Biol. Chem.* 280:14145–14153. doi:10.1074/jbc.M500901200

Storer, P.D., J. Xu, J. Chavis, and P.D. Drew. 2005. Peroxisome proliferator-activated receptor-gamma agonists inhibit the activation of microglia and astrocytes: implications for multiple sclerosis. *J. Neuroimmunol.* 161:113–122. doi:10.1016/j.jneuroim.2004.12.015

Straus, D.S., and C.K. Glass. 2007. Anti-inflammatory actions of PPAR ligands: new insights on cellular and molecular mechanisms. *Trends Immunol.* 28:551–558. doi:10.1016/j.it.2007.09.003

Stromnes, I.M., L.M. Cerretti, D. Liggitt, R.A. Harris, and J.M. Goverman. 2008. Differential regulation of central nervous system autoimmunity by T(H)1 and T(H)17 cells. *Nat. Med.* 14:337–342. doi:10.1038/nm1715

Windhagen, A., J. Newcombe, F. Dangond, C. Strand, M.N. Woodroofe, M.L. Cuzner, and D.A. Hafler. 1995. Expression of costimulatory molecules B7-1 (CD80), B7-2 (CD86), and interleukin 12 cytokine in multiple sclerosis lesions. *J. Exp. Med.* 182:1985–1996. doi:10.1084/jem.182.6.1985

Yang, Y., J. Weiner, Y. Liu, A.J. Smith, D.J. Huss, R. Winger, H. Peng, P.D. Cravens, M.K. Racke, and A.E. Lovett-Racke. 2009. T-bet is essential for encephalitogenicity of both Th1 and Th17 cells. *J. Exp. Med.* 206:1549–1564. doi:10.1084/jem.20082584